

Journal of Bioscience and Bioengineering
VOL. xxx No. xxx, xxx, xxxx

www.elsevier.com/locate/jbiosc

Development of nucleic acid based lateral flow assays for SARS-CoV-2 detection

Dilek Çam Derin,[1,*] Enes Gültekin,[1] Irmak İçen Taşkın,[1] and Yusuf Yakupoğulları[2]

Department of Molecular Biology and Genetics, Inonu University, 44280 Malatya, Turkey[1] *and Department of Medical Microbiology, Inonu University, 44280 Malatya, Turkey*[2]

Received 30 August 2022; accepted 1 November 2022
Available online xxx

SARS-CoV-2 is still threat for humanity and its detection is crucial. Although real time reverse transcriptase polymerase chain reaction is the most reliable method for detection of N protein genes, alternative methods for molecular detection are still needed. Thus, lateral flow assay models for 2019-nCoV_ N3 were developed for molecular detection. Briefly, gold nanoparticles were used as label and three sandwich models (1A, 1B, and 1.2) were designed. Prob concentrations on gold nanoparticles, types of sandwich model and membrane, limit of detection of target gene and buffer efficiency were studied. Model 1B has shown the best results with M170 membrane. Lower limit of detection was achieved by model 1.2 as 5 pM. All parameters have significant role for molecular detection of SARS-CoV-2 by lateral flow assays, and these results will be useful for nucleic acid based lateral flow assays for viral detection or multiple detection of mutated forms in various detection systems.

© 2022, The Society for Biotechnology, Japan. All rights reserved.

[**Keywords:** Rapid test; SARS-CoV-2; Sandwich assay; 2019-nCoV_N; Detection]

Wuhan viral pneumonia seen in the late 2019 was called as SARS-CoV-2 and COVID-19 caused by SARS-CoV-2 was named as disease by World Health Organization (WHO). SARS-CoV-2 is an RNA virus belonging to the β and it has at least four structural proteins including spike (S) protein, envelope (E) protein, membrane (M) protein and nucleocapsid (N) protein. S protein is widely used for diagnosis because of antigenicity and commonly chosen as target for neutralizing antibodies. However, N protein becomes attractive for molecular diagnosis of COVID-19 as highly protected protein sequences and high immunogenicity (1). Additionally, N protein is abundantly expressed protein during the infection and causes to protective immune response for SARS CoV and COVID-19 (2). The sequence similarity of protein coding region of COVID-19 was found as 89.74%, 48.59% and 35.62% with SARS CoV, MERS-CoV and HCoV-OC43, respectively (3) and 96% with bat coronavirus in the whole genom level (1). The comprehensive domain structure of N proteins among the four coronaviruses (SARS-CoV-2, SARS-CoV, MERS-CoV, and HCoV-OC43) and the complete genome of SARS-CoV-2 were reported in the literature (3). To say that the characteristics of the surface electrostatic potential of N terminal domain of SARS-CoV-2 N protein is different even if it is similar to the other coronaviruses.

N region of SARS-CoV-2 was determined as target sequence for SARS-CoV-2 specific gene. WHO proposed a few primer sets for N gene and reported that 2019-nCoV_ N3 (USA) and NIID_2019-nCOV_N (Japan) primers are the most sensitive for real time reverse transcription polymerase chain reaction (rRT-PCR) (4). Therefore, among the specific regions N gene regions are widely accepted for diagnosis as the high similarity between SARS-CoV-2 and SARS-CoV causes to mistake in molecular diagnosis. SARS-CoV-2 RNA may be obtained from bronchoalveolar lavage, nasal/pharingeal swab (53.6%–73.3%) (5), salivary/sputum (74.4%–88.9%) (6), feces/urine, blood samples and anal/oral swabs (7–9). Additionally, it is known that virus may be alive at suitable environmental conditions after leaving from human body and join to waste water. Thus, SARS-CoV-2 and newly developed coronaviruses will always threaten the public health since the development of antiviral drugs or therapeutics takes long time. In this reason, early molecular viral detection is crucial to get under control the epidemy/pandemia.

Serology is a standart method for viral detection and based on the testing of antibody response coming from the immune system and antigen presence. However, it cannot be used for early detection since it is based on the measurement of antibody after infection, and could not be efficient for patients who are in risk groups. For instance, antibodies against to COVID-19 are developed in early stage (4–10 days for IgM) and late stage (11–24 days for IgM–IgG). Besides, cross antibody reactions may give a false positive result and producing of polyclonal antibodies may change from batch to batch. Nanoparticle based viral diagnosis (10) is another way and it was used for the detection of SARS specific sequence (11). However, there is lack of nano-based diagnosis systems for SARS-CoV-2 sequences even if antigen based detections are reported (12–17). rRT-PCR is the most reliable method for molecular detection of SARS-CoV-2 in the world and the first quantitative rRT-PCR was designed after the definition of virus by WHO in January 2020. Although these assays are reliable, complex and expensive test protocols, need of educated personnel and diagnosis laboratories, taking time for sending the samples into reference labs are disadvantages. Similarly, conventional PCR needs agarose gel loading and high copy number of target genes. For these reasons, rapid and

* Corresponding author.
E-mail addresses: cam.dilek@gmail.com (D. Çam Derin), enesgultekin1461@gmail.com (E. Gültekin), irmak.taskin@inonu.edu.tr (I. İçen Taşkın), yusuf.yakupogullari@inonu.edu.tr (Y. Yakupoğulları).

1389-1723/$ – see front matter © 2022, The Society for Biotechnology, Japan. All rights reserved.
https://doi.org/10.1016/j.jbiosc.2022.11.001

naked-eye molecular detection of SARS-CoV-2 is always needed. In this regard, lateral flow assays (LFAs) or point of care tests could be an alternative to the molecular detection of SARS-CoV-2 as a rapid, cheap and simple way without advanced devices in a short time.

LFAs are portable, ready to use immunochromatographic diagnostic assays developed by antibodies, enzymes or nucleic acids (18) for various fields. They can also be helpful for epidemy/pandemia by sensitive detection of nucleic acids (19) and could make 8 times sensitive and rapid detection compared to the electrophoresis (20). While a number of LFAs were developed for COVID-19, they are mostly based on the antibody (IgG/IgM) detection of patients (21) and there is lack of nucleic acid detection of SARS-CoV-2 by LFAs. LFAs can be used with amplification systems producing any RNA (22). Although LFA for molecular detection of SARS-CoV-2 is reported in the literature, it is based on CRISPR Cas12a dependent nucleic acid detection (23) and needs the complex experimental steps. Similarly, Broughton et al. (24) developed the LFAs for SARS-CoV-2 using the RNA extracts related with respiratory swab. It is based on the CRISPR–Cas12 for the detection of E and N gene (24). However, extra labelling with fluorescein amidites and sensitive steps including enzymatic restriction are needed, and assay was only developed for one region of N gene announced by US Centers for Disease Control and Prevention which are accepted regions for rRT-PCR. LFAs are encouraged to be developed for nucleic acid detection of SARS-CoV-2 based on PCR. Therefore, nucleic acid-based LFAs that can adopt new sequences generated by viral mutations are always important.

In this research, molecular detection of RNA region (2019-nCoV_N3) specific to SARS-CoV-2 by gold nanoparticles (AuNPs) based LFAs in 5–7 min was aimed. Test principle is based on the hybridization of oligonucleotides without complex enzymatic reactions and naked-eye analysis.

MATERIALS AND METHODS

The chemicals used were all analytical grades. $HAuCl_4 \cdot 3H_2O$ and trisodium citrate dihydrate were purchased from Alfa Aesar (Kandel, Germany). Ultra-low range DNA ladder was from Thermo Scientific (Waltham, MA, USA). Tris–HCl was purchased from AppliChem (Darmstadt, Germany), KCl and NaCl were purchased from Merck (Darmstadt, Germany), $MgCl_2$, $CaCl_2$, nuclease free water and SSC buffer were purchased from Multicell (Lawrenceville, GA, USA). Tris(2-carboxyethyl) phosphine hydrochloride (TCEP) was purchased from Sigma Aldrich (St. Louis, MO, USA). Synthetic oligonucleotides were purchased from Integrated DNA Technologies (Coralville, IA, USA). Ultrapure water was used for the preparation of all solutions during the study. The nitrocellulose membrane cards were purchased from Whatman, GE Healthcare, Dassel, Germany. Absorbent pad, sample pad and conjugate pad were purchased from Millipore, Burlington, MA, USA. Scanning transmission electron microscope (STEM, TESCAN, Sivas, Turkey), Horiba Dynamic Laser Particle Size/Zeta Potential Analyzer (Horiba, Kyoto, Japan) and Epoch 2 Plate Reader/Spectrophotometer (BioTek, Malatya, Turkey) were used for analysis of synthesized AuNPs and AuNPs/prob concentration. As a probe 1A model: GNP probe 1A: 5′ cca atg tga tct ttt ggt gta aaa aaa aaa-3 -SH′; test line for 1A: 5′bio aaa aaa a gca ttg tta gca gga ttg c 3′ and control line for 1A: 5′ tac acc aaa aga tca cat tgg ttt 3′bio were used. As a probe 1B model: GNP probe 1B: 5′ ttt ggt gta ttc aag gct ccc aaa aaa aaa-3 -SH'; test line for 1B: 5′bio aaa aaa tg cgg gtg cca atg tga tct 3′ and control line for 1B: 5′ ggg agc ctt gaa tac acc aaa ttt 3′bio were used. As a probe 1.2 model: GNP probe 1.2: 5′ t gcc aat gtg atc ttt tgg tg aaa aaa aaa-3 -SH′; test line for 1.2: 5′bio aaa aaa gc agc att gtt agc agg att 3′ and control line for 1.2: 5′ ca cca aaa gat cac att ggc a ttt 3'bio were used. 2019-nCoV_N3 which is 72 base long target N gene region 1, 5′-ggg agc ctt gaa tac acc aaa aga tca cat tgg cac ccg caa tcc tgc taa caa tgc tgc aat cgt gct aca-3′, and 50 base long target N gene region 1.2 (2019-nCoV_N3), 5′ aat aca cca aaa gat cac att ggc acc cgc aat cct gct aac aat gct gc -3′, were experienced. 5′ggg agc ctt gaa tac acc aaa a 3′ and 5′tgt agc acg att gca gca ttg 3′ primers were used as forward and reverse, respectively, for PCR reaction.

Synthesis of gold nanoparticles and conjugation with oligonucleotide probes AuNPs were synthesized by reducing the $HAuCl_4 \cdot 3H_2O$ with sodium citrate (25), in conical flask. All the glass materials used were cleaned with acid solution and rinsed with distilled water. Briefly, 100 mL of 1 mM $HAuCl_4 \cdot 3H_2O$ solution was boiled by stirring continuously. Then 1% sodium citrate was added and the color changed from black to red in 2–3 min. Boiling was continued about 10 min and colloidal solution was allowed to cool. Synthesized AuNPs were filtered by 0.45 μm cellulose acetate and concentrated by centrifugation at four times (4X AuNPs) before the conjugation with oligonucleotides and stored at 4 °C. To make a conjugate with oligonucleotide probes, thiol modified probes were initially activated by TCEP for 1 h at room temperature. In this purpose, three probe concentrations (2, 4, and 8 μM) were used for conjugation in order to see the effect of probe concentration on assay efficiency. Then solution was added into 1 mL of 4X AuNPs solution and incubated for overnight at room temperature. After that 0.01 M phosphate buffer saline (PBS) was added as final concentration for salt aging and incubated for overnight. Then, the solution was centrifuged at 12,000 rpm and pellet was resuspended in resuspension buffer (20 mM sodium phosphate buffer containing 5% BSA, 0.25 % Tween 20 and sucrose). Conjugate was washed with the resuspension buffer as twice and stored at 4 °C after resuspending in the same buffer.

Preparation of LFAs The components of the LFAs are sample pad, conjugate pad, nitrocellulose membrane and absorbent pad. The design of strip assay was manually performed according to our previous study (26). Two different cellulose membranes having different flow rates were used in this study (M170-M120). In short, sample pads were treated with two different buffers called as buffer 4 (0.05 M Tris–HCl, 0.25% Triton X-100, 0.15 M NaCl, pH 8.0) and buffer 5 (PBS, 0.1 mM NaCl, 0.2 % Tween 20), separately and dried at 37 °C or room temperature. Conjugate pads were soaked with AuNPs/Probe conjugate and dried at 37 °C for 1 h. Buffer 14 (20 mM Tris, 50 mM NaCl, 5 mM KCl, 5 mM MgCl2, 2 mM CaCl2, 0.1 mM BSA, 1.7% Triton X-100, pH 8.0), PBS and saline-sodium citrate (SSC) was used as running buffer for optimizing the assay. Test and control lines are prepared by the principle of streptavidin-biotin interaction. Briefly, biotinylated oligonucleotides were conjugated to streptavidin and then immobilized on the cellulose membrane using micropipette manually. For the assay development three sandwich models (1A, 1B, and 1.2) were prepared for hybridization on LFA and experienced separately. Two of them (1A and 1B) were for 72 base long 2019-nCoV_N3 and the last one (1.2) was for 50 base long which was obtained from shortening the 2019-nCoV_N3 region which is still specific for SARS-CoV-2.

Polimerase chain reaction for 2019-nCoV_N3 In order to see the application potential of developed LFAs for real samples, PCR was performed by plasmid DNA including N gene of SARS-CoV-2 and specific primers for 2019-nCoV_N3. After the reaction was completed, PCR product was run on agarose gel electrophoresis along with the Ultra-low DNA ladder at 90V for 1 h to be sure that correct gene region was obtained before applying to the LFA. The PCR reaction was performed as 34 cycle for each tube and finally extended as 72 °C for 4 min. PCR products were heated for denaturation and then applied to the strip assays.

RESULTS AND DISCUSSION

Synthesis of gold nanoparticles and conjugation with oligonucleotide probes Synthesized AuNPs were analyzed by STEM, UV–Vis spectroscopy and Dynamic Laser Particle Size Analyzer. According to the analysis, homogenously distributed spherical colloidal AuNPs were measured as about 13 nm and λ_{max} was 521 nm as expected (Fig. S1). Additionally, the measurement of STEM analysis showed that value: l [nm], objective count: 85, summation: 1071.01, minimum value: 9.44, maximum value: 20.26, mean value: 12.60 and standard deviation: 2.21. The concentration of synthesized AuNPs was also calculated as 0.4 nM according to the extinction coefficient of 13 nm at 521 nm wavelength (27).

After the conjugation of AuNPs with thiol modified probes, their max absorption peaks were shifted from 521 to 526 nm as expected (Fig. S2). This is because in the three sandwich models, the coating of AuNPs by the probes (4 μM and 8 μM) changed the surface charge of the AuNPs and shifted the maximum absorption peak. While the concentration of probes on AuNPs was enough for 4 and 8 μM for three models, 2 μM probe was not enough for sustaining the stability of AuNPs since it caused the aggregation of AuNPs (data not shown). Therefore, 4 and 8 μM coated AuNPs were used for further studies for three LFA models.

Preparation of LFA models The components of LFAs were manually prepared and three sandwich models (1A, 1B, and 1.2) (Fig. S3) were applied to assay separately. These models were designed to make comparison between the models and find the best one for molecular recognition of SARS-CoV-2 by LFAs.

Agarose gel electrophoresis of 2019-nCoV_N3 PCR PCR was performed by using plasmid DNA including N gene and primers specific for 2019-nCoV_N3 were used for amplification of 72 bp

Please cite this article as: Çam Derin, D et al., Development of nucleic acid based lateral flow assays for SARS-CoV-2 detection, J. Biosci. Bioeng., https://doi.org/10.1016/j.jbiosc.2022.11.001

target. This was made for verification of presenting the target gene in our sample and mimicking the real PCR samples coming from the patients, which will be applied to the LFAs for further studies. PCR products for 2019-nCoV_N3 (72 bp) are shown in Fig. S4.

Application of targets to the LFAs models Here probe concentration on AuNPs, sandwich models, membrane types, limit of detection (LOD) of target gene and buffer efficiency for molecular detection of 2019-nCoV_N3 on designed LFAs were studied. LFAs were prepared by four membranes and target was used as synthetic oligonucleotide sequence of 2019-nCoV_N3. Initially, buffer optimizations were experienced. For this purpose, sample pads were soaked with two buffers, buffer 4 and buffer 5, and three different buffers, buffer 14, PBS and SSC were used as running buffer. Under these conditions, the LFA control line should always appear red, and both the test line and the control line should appear red in order to say that the test is positive. Results verified that membrane type and designed models have significant differences when they are used with different buffers and temperatures (data not shown). For instance, model 1B has shown the best results with M170 membrane compared to the M120 membrane for using 4 μM and 8 μM probe concentrations at 37 °C drying (Fig. 1, B1–10 and D1–4), while the model 1A has weak test lines with M170 and M120 membranes at the same temperature (Fig. 1, A1–10 and C1–4). Although there are no significant differences between buffer 4 and 5 for assay results, SSC buffer was used for further studies as it has clear red color intensity on both the test and control lines and showed no nonspecific bindings on LFAs for all models using 4 and 8 μM probe concentrations. This finding is meaningful as SSC buffer has commonly positive effect on oligonucleotide hybridizations. To highlight, all developed strips have selectively detected the target and showed no nonspecific binding to the Mers CoV_N2, Mers CoV_N3 and RdRp/Orf1 sequences of SARS CoV_2, which are specific for Mers CoV and SARS-CoV-2, respectively. This means that the designed LFA strips are suitable and reliable for molecular detection of SARS-CoV-2. Additionally, all strip assays worked truely since all the control lines are visible even if two of them are weak in positive assay (Fig. 1, A1 and C1). This is probably caused by the weak interaction between the capture and detection reagent for prob 1A.

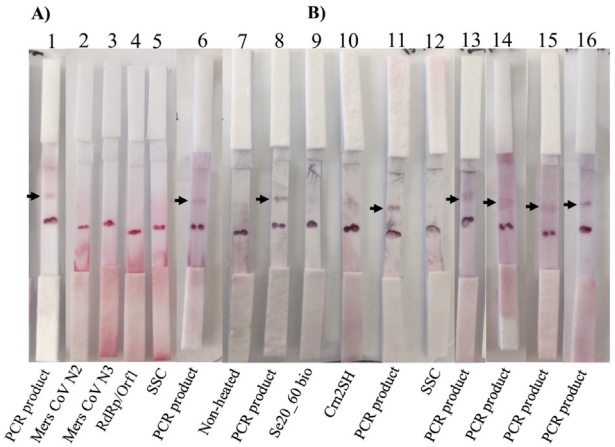

FIG. 2. Application of PCR products to LFAs developed by two types of membranes and three models. (A) Strips 1–8 were prepared by 4 μM and (B) strips 9–16 were prepared by 8 μM. Strips 1–15 were prepared by M170 and strip 16 was prepared by M120 membrane. Strips 1–5: model 1.2, strips 6–13 and 16: model 1B, strips 14 and 15: model 1A. Non-heated: non-heated PCR product. Se20_60 bio, Crn2SH, Mers CoV_N2, Mers CoV_N3 and RdRp/Orf1 and SSC are negative controls. Arrows show the test lines.

Application of PCR products to LFAs designed by three models PCR products were applied to the developed LFAs using three models and two type of membranes. To make sure that for selective detection of target, random oligonucleotide sequences such as Se20_60 bio, Crn2SH and Mers CoV_N2, Mers CoV_N3 and RdRp/Orf1 of SARS-CoV-2, SSC running buffer were used as negative controls. Findings showed that all models recognized the target sequence, selectively without any nonspecific bindings of negative controls (Fig. 2). Although there is no significant differences between the strip assays, model 1B on both membranes might be considered as the best for the detection of 2019-nCoV_N3 in PCR sample by two probe concentrations (Fig. 2, strips 6, 8, 11, and 16). Although the test line intensity on model 1.2 (Fig. 2, A1) and model 1A (Fig. 2, B14–B15) is weak compared to model 1B, they could make selective detection without any nonspecific binding to the negative controls (Fig. 1A and C and Fig. 2, A2–A5).

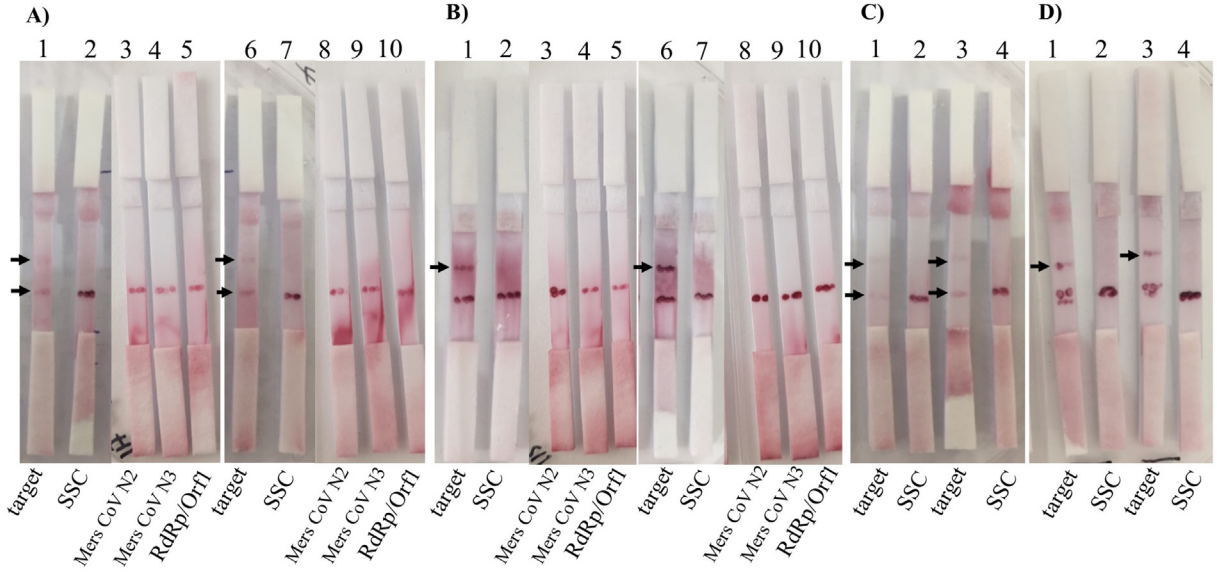

FIG. 1. LFAs developed by M170 (A, B) and M120 membrane (C, D) using model 1A (A, C) and model 1B (B, D) at 37 °C drying. Strips A1–A5, B1–B5, C1–C2, and D1–D2 were prepared by 4 μM probe and strips A6–A10, B6–B10, C3–C4, and D3–D4 were prepared by 8 μM probe. Target: 2019-nCoV_N3 (72 bp), SSC: running buffer. Arrows show the test and control lines.

Please cite this article as: Çam Derin, D et al., Development of nucleic acid based lateral flow assays for SARS-CoV-2 detection, J. Biosci. Bioeng., https://doi.org/10.1016/j.jbiosc.2022.11.001

ARTICLE IN PRESS

Briefly, all these results mean that designed assay models could be good candidate for naked-eye analysis of SARS-CoV-2 without advanced rRT-PCR devices and agarose gel electrophoresis. In addition, the developed LFA is considered advantageous and more sensitive than conventional agarose gel electrophoresis because it carries a very small amount of PCR products (5 μL). This is because agarose gel electrophoresis requires a large amount of PCR product and a long analysis time. There was no significant difference in the detection of PCR products between the two probe concentrations (4 μM–8 μM).

Limit of detection of LFAs designed by three models LOD experiments were performed by using synthetic target with developed LFAs by three sandwich models and two membrane types. It is clearly seen that model 1A works efficiently since the control lines of all strips are seen and the results showed that 0.1 μM target (72 base long) was sensitively recognized by model 1A using both membrane types (Fig. 3, B3 and D1, D3). Interestingly, there is significant difference in terms of the detection of this amount by M120 membrane. The line intensities of 0.5 μM target (Fig. 3C) are weak compared to the 0.1 μM target (Fig. 3D).

It might be said that the sensitivity of LFAs based on hybridization is significantly affected by the amount of target and membrane type. It means that there is an optimum concentration between the capture and detection oligonucleotides for effective hybridization and it is not directly related with high amount of target for this model designed with this membrane. However, the line intensities on M170 membrane were gradually become weak when the concentration of target was decreased for two probe concentrations (Fig. 3A and B). While the LOD is 0.1 μM target by using 8 μM probe (Fig. 3B, strip 3), it was 0.5 μM using 4 μM probe on this membrane. These findings suggested that probe concentrations on AuNPs have significant role for sensitive detection along with the membrane type. This can also be verified by comparing the strips developed by 4 μM probes with M170 (Fig. 3B, strip 1) and M120 membrane (Fig. 3D, strip 1) for the same LOD.

LOD experiments were experienced by model 1B using both membranes and two probe concentrations (Fig. 4). According to the results, 0.1 μM target (72 base long) was detected by M170 membrane using both probe concentrations (Fig. 4B) while it was 0.005 μM by M120 membrane using 8 μM probe (Fig. 4F). These results verified that membrane types and probe concentrations used in LFAs have significant role for sensitive detection. Here, the sandwich model, another important aspect of high-sensitivity detection, appears to be superior to model 1A, as all strips have clear line intensities and low detection limits.

LOD was also experienced by model 1.2 using both membranes and two probe concentrations (Fig. 5). According to the results the minimum amount of target, 50 base long, was detected as 5 pM by M170 membrane using 8 μM probe (Fig. 5C, strip 1) while it was 100 pM by M120 membrane using 8 μM probe concentration (Fig. 5E, strip 3) without any nonspecific bindings. This amount is either lower than the reported nucleic acid based LFAs (28,29) or similar with the amount of SARS CoV_2 N protein detection (30). Thus, to make sensitive recognition, 8 μM probe could be used for this model. Lastly, model 1.2 allowed effective hybridization on both lines and this was resulted by clear line intensity and the lowest detection amount of target.

When compared to all models in terms of the LOD, the length of the target has crucial role for LFA efficiency. It could be inferred from these results 50 base long target sequence could be sensitively recognized compared to the 72 base long as the base length of target sequence become shorter, LOD was observed as lower. This may be caused by the high probability of the hairpin structures in long bases, which can interfere the hybridization on the assay. Therefore, sensitive detection is closely related with the length of target sequence and hybridization models between the target and capture reagents for LFA. Along with this, it should be highlighted that the main gene length (72 base long) is also clearly detected by developed strip assay models and could be used for the detection of 2019-nCoV_N3.

Lastly, LFAs were also prepared by different times in order to see the stability of conjugates and LFAs efficiency. Therefore, assays were applied by 6 months awaited conjugates. It was found that conjugates were still stable and worked efficiently in terms of the hybridization on the LFAs and both lines on the strips were clearly observed (data not shown). Since the stability of the conjugates is also highly related with the red color of suspension, they still have their original color (data not shown). Therefore, designed LFAs with these models have potential for long shelf life if they are fabricated. Because the developed method is also consistent in terms of the reproducibility and there was no difference in batch to batch production or preparation of all LFA strips.

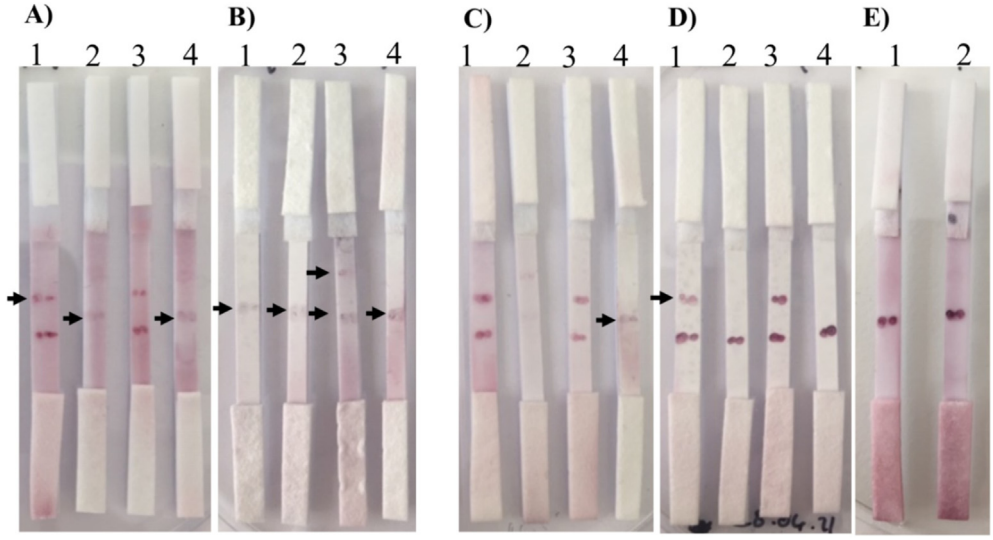

FIG. 3. LOD of target by model 1A using M170 (A, B) and M120 (C–E). (A) 0.5 μM, (B) 0.1 μM, (C) 0.5 μM, (D) 0.1 μM, (E) 0.005 μM target. Strips 1 and 2 were prepared by 4 μM probe and strips 3 and 4 were by 8 μM. Strip E1 was prepared by 4 μM and E2 was by 8 μM, and then target was applied to both. Strips 1–3 were all applied by target and strips 2–4 were by buffer as a negative control. Arrows show the test and control lines.

Please cite this article as: Çam Derin, D et al., Development of nucleic acid based lateral flow assays for SARS-CoV-2 detection, J. Biosci. Bioeng., https://doi.org/10.1016/j.jbiosc.2022.11.001

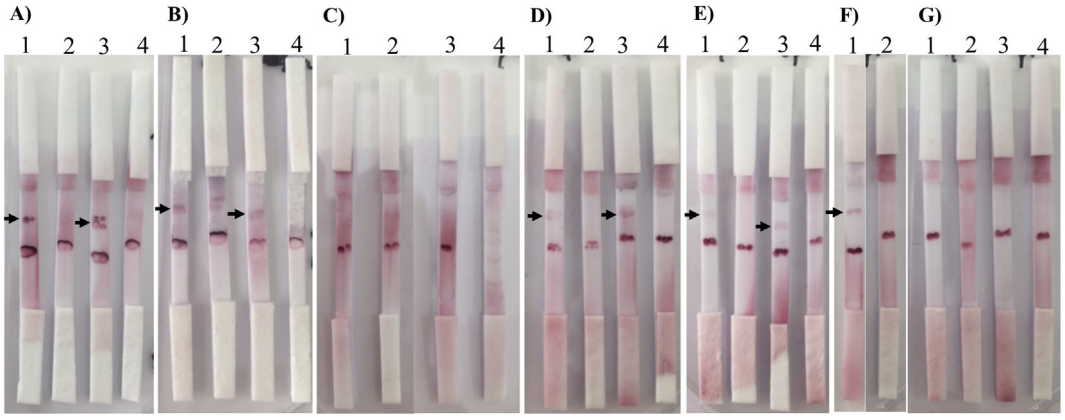

FIG. 4. LOD of target by model 1B using M170 (A–C) and M120 (D–G). (A) 0.5 μM, (B) 0.1 μM, (C) 100 pM, (D) 0.5 μM, (E) 0.1 μM, (F) 0.005 μM, (G) 100 pM target. Strips 1 and 2 were prepared by 4 μM probe and strips 3 and 4 were by 8 μM. Strips F1 and F2 were prepared by 8 μM. Strips 1–3 were all applied by target and strips 2–4 were by buffer as a negative control. Arrows show the test lines.

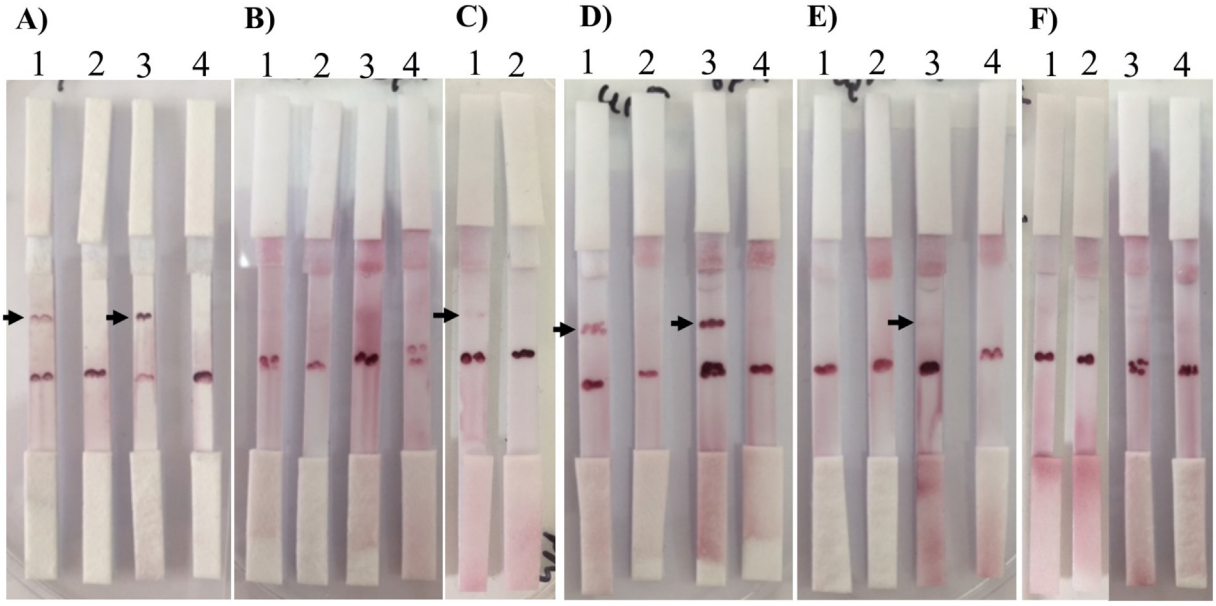

FIG. 5. LOD of target by model 1.2 using M170 (A–C) and M120 (D–F). (A) 0.005 μM, (B) 50 pM, (C) 5 pM, (D) 0.005 μM, (E) 100 pM, (F) 50 pM target. Strips 1–2 were prepared by 4 μM prob and strips 3–4 were by 8 μM. Strips C1–C2 were prepared by 8 μM. All 1–3 strips were applied by target and strips 2–4 were by buffer as a negative control. Arrows show the test lines.

As a conclusion, the detection of SARS-CoV-2 by targeting the 2019-nCoV_N3 gene region was succeeded by designed LFAs models as a first study according to the best of our knowledge. Although the detection of virus by LFAs is commonly based on the immunoglobulins of patients or antigens, these models are for the molecular detection of SARS-CoV-2 since it is the most reliable method in the world. LFA is cost-effective because it can be analyzed by the naked eye, allowing conventional PCR products to be used instead of expensive analyzers and reagents such as rRT-PCR. We believe that findings will be valuable for various molecular detection methods for SARS-CoV-2 and its mutants. Because assay is based on the hybridization and can be rapidly designed for specific sequences of mutant viruses. Thus, the detection of either mutated or conserved regions could be possible by these type of assay models. Since the PCR products were recognized and parameters were optimized in designed LFAs they might also be a candidate for point of care diagnosis in terms of the molecular detection of SARS-CoV-2 for further fabrication. In this perspective, applying the developed LFAs to the real samples coming from the patients will be planned for the future work.

Supplementary data to this article can be found online at https://doi.org/10.1016/j.jbiosc.2022.11.001.

ACKNOWLEDGMENTS

This work was supported by Inonu University Scientific Research Project (BAP; TOA-2020-2238).

References

1. **Zhou, P., Yang, X. L., Wang, X. G., Hu, B., Zhang, L., Zhang, W., Si, H. R., Zhu, Y., Li, B., Huang, C. L., Chen, H. D., and Chen, J.:** A pneumonia outbreak associated with a new coronavirus of probable bat origin, Nature, **579**, 270–273 (2020).
2. **Ahmed, S. F., Quadeer, A. A., and McKay, M. R.:** Preliminary identification of potential vaccine targets for the COVID-19 coronavirus (SARS-CoV-2) based on SARS-CoV immunological studies, Viruses, **12**, 254 (2020).

ARTICLE IN PRESS

3. **Kang, S., Yang, M., Hong, Z., Zhang, L., Huang, Z., Chen, X., He, S., Zhou, Z., Zhou, Z., Chen, Q., Yan, Y., and Zhan, C.:** Crystal structure of SARS-CoV-2 nucleocapsid protein RNA binding domain reveals potential unique drug targeting sites, Acta Pharm. Sin. B, **10**, 1228–1238 (2020).
4. **Jung, Y.,, Park, G. S., Moon, J. H., Ku, K., Beak, S. H., Lee, C. S., Kim, S., Park, E. C., Park, D., Lee, J. H., Byeon, C. W., and Lee, J. J.:** Comparative analysis of primer–probe sets for RT-qPCR of COVID-19 causative virus (SARS-CoV-2), ACS Infect. Dis., **6**, 2513–2523 (2020).
5. **Huang, C., Wang, Y., Li, X., Ren, L., Zhao, J., Hu, Y., Zhang, L., Fan, G., Xu, J., Gu, X., Cheng, Z., and Yu, T.:** Clinical features of patients infected with 2019 novel coronavirus in Wuhan, China, Lancet, **395**, 497–506 (2020).
6. **Yang, Y., Yang, M., Yuan, J., Wang, F., Wang, Z., Li, J., Zhang, M., Xing, L., Wei, J., Peng, L., Wong, G., and Zheng, H.:** Comparative sensitivity of different respiratory specimen types for molecular diagnosis and monitoring of SARS-CoV-2 shedding in COVID-19 patients, Innovation, **1**, 3 (2020).
7. **Zhang, W., Du, R. H., Li, B., Zheng, X. S., Yang, X. L., Hu, B., Wang, Y. Y., Xiao, G. F., Yan, B., Shi, Z. L., and Zhou, P.:** Molecular and serological investigation of 2019-nCoV infected patients: implication of multiple shedding routes, Emerg. Microbes Infect., **9**, 386–389 (2020).
8. **Holshue, M. L., DeBolt, C., Lindquist, S., Lofy, K. H., Wiesman, J., Bruce, H., Spitters, C., Ericson, K., Wilkerson, S., Tural, A., Diaz, G., and Cohn, A.:** First case of 2019 novel coronavirus in the United States, N. Engl. J. Med, **382**, 929–936 (2020).
9. **Pan, Y., Zhang, D., Yang, P., Poon, L. L. M., and Wang, Q.:** Viral load of SARS-CoV-2 in clinical samples, Lancet Infect. Dis, **20**, 411–412 (2020).
10. **Wang, X., Liu, L. H., Ramstroem, O., and Yan, M.:** Engineering nanomaterial surfaces for biomedical applications, Exp. Biol. Med. (Maywood), **234**, 1128–1139 (2009).
11. **Martínez-Paredes, G., González-García, M. B., and Costa-García, A.:** Genosensor for SARS virus detection based on gold nanostructured screen-printed carbon electrodes, Electroanalysis, **21**, 379–385 (2009).
12. **Mahari, S., Roberts, A., Shahdeo, D., and Gandhi, S.:** eCovSens-ultrasensitive novel in-house built printed circuit board based electrochemical device for rapid detection of nCovid-19 antigen, a spike protein domain 1 of SARS-CoV-2, BioRxiv, https://doi.org/10.1101/2020.04.24.059204 (2020).
13. **Roberts, A., Mahari, S., Shahdeo, D., and Gandhi, S.:** Label-free detection of SARS-CoV-2 Spike S1 antigen triggered by electroactive gold nanoparticles on antibody coated fluorine-doped tin oxide (FTO) electrode, Anal. Chim. Acta, **1188**, 339207 (2021).
14. **Shahdeoa, D., Robertsa, A., Archana, G. J., Shrikrishna, S. N., Mahari, S., Nagamani, K., and Gandhi, S.:** Label free detection of SARS CoV-2 receptor binding domain (RBD) protein by fabrication of gold nanorods deposited on electrochemical immunosensor, Biosens. Bioelectron., **212**, 114406 (2022).
15. **Shahdeo, D., Chauhan, N., Majumdar, A., Ghosh, A., and Gandhi, S.:** Graphene-based field-effect transistor for ultrasensitive immunosensing of SARS-CoV-2 spike S1 antigen, ACS Appl. Bio Mater., **5**, 3563–3572 (2022).
16. **Ligieroa, C. B. P., Fernandes, T. S., D'Amato, D. L., Gaspar, F. V., Duarte, P. S., Strauch, M. A., Fonseca, J. G., Meirelles, L. G. R., Silva, P. B., Azevedo, R. B., Martins, G. A. S., Archanjo, B. S., and other 4 authors:** Influence of particle size on the SARS-CoV-2 spike protein detection using IgG-capped gold nanoparticles and dynamic light scattering, Mater. Today Chem., **25**, 100924 (2022).
17. **DaSilva, P. B., DaSilva, J. R., Rodrigues, M. C., Vieira, J. A., Andrade, I. A., Nagata, T., and Santos, A. S.:** Detection of SARS-CoV-2 virus via dynamic light scattering using antibody-gold nanoparticle bioconjugates against viral spike protein, Talanta, **243**, 123355 (2022).
18. **Ang, G. Y., Yu, C. Y., and Yean, C. Y.:** Ambient temperature detection of PCR amplicons with a novel sequence-specific nucleic acid lateral flow biosensor, Biosens. Bioelectron, **38**, 151–156 (2012).
19. **Reboud, J., Xu, G., Garrett, A., Adriko, M., Yang, Z., Tukahebwa, E. M., Rowell, C., and Cooper, J. M.:** Paper-based microfluidics for DNA diagnostics of malaria in low resource underserved rural communities, Proc. Natl. Acad. Sci. USA, **116**, 4834–4842 (2019).
20. **Glynou, K., Ioannou, P. C., Christopoulos, T. K., and Syriopoulou, V.:** Oligonucleotide-functionalized gold nanoparticles as probes in a dry-reagent strip biosensor for DNA analysis by hybridization, Anal. Chem, **75**, 4155–4160 (2003).
21. **Li, Z., Yi, Y., Luo, X., Xiong, N., Liu, Y., Li, S., Sun, R., Wang, Y., Hu, B., Chen, W., Zhang, Y., and Wang, J.:** Development and clinical application of a rapid IgM-IgG combined antibody test for SARS-CoV-2 infection diagnosis, J. Med. Virol., **92**, 1518–1524 (2020).
22. **Dimov, I. K., Garcia-Cordero, J. L., O'Grady, J., Poulsen, C. R., Viguier, C., Kent, L., Daly, P., Lincoln, B., Maher, M., O'Kennedy, R., Smith, T. J., and Ricco, A. J.:** Integrated microfluidic tmRNA purification and real-time NASBA device for molecular diagnostics, Lab Chip, **8**, 2071–2078 (2008).
23. **Lucia, C., Federico, P. B., and Alejandra, G. C.:** An ultrasensitive, rapid, and portable coronavirus 2 SARS-CoV-2 sequence detection method based on CRISPR-Cas12, BioRxiv, https://doi.org/10.1101/2020.02.29.971127 (2020).
24. **Broughton, J. P., Deng, X., Yu, G., Fasching, C. L., Servellita, V., Singh, J., Miao, X., Streithorst, J. A., Granados, A., Gonzalez, A. S., Zorn, K., and Gopez, A.:** CRISPR–Cas12-based detection of SARS-CoV-2, Nat. Biotechnol, **38**, 870–874 (2020).
25. **Grabar, K. C., Freeman, R. G., Hommer, M. B., and Natan, M. J.:** Preparation and characterization of Au colloid monolayers, Anal. Chem, **67**, 735–743 (1995).
26. **Cam, D. and Oktem, H. A.:** Development of rapid dipstick assay for food pathogens, Salmonella, by optimized parameters, J. Food Sci. Technol., **56**, 140–148 (2019).
27. **Zhao, W., Brook, M. A., and Li, Y.:** Design of gold nanoparticle-based colorimetric biosensing assays, Chembiochem, **9**, 2363–2371 (2008).
28. **Jauset-Rubio, M., Svobodová, M., Mairal, T., McNeil, C., Keegan, N., Saeed, A., Abbas, M. N., El-Shahawi, M. S., Bashammakh, A. S., Alyoubi, A. O., and OSullivan, C. K.:** Ultrasensitive, rapid and inexpensive detection of DNA using paper based lateral flow assay, Sci. Rep., **6**, 37732 (2016).
29. **Baeumner, A. J., Pretz, J., and Fang, S.:** A universal nucleic acid sequence biosensor with nanomolar detection limits, Anal. Chem., **76**, 888–894 (2004).
30. **Grant, B. D., Anderson, C. E., Williford, J. R., Alonzo, L. F., Glukhova, V. A., Boyle, D. S., Weigl, B. H., and Nichols, K. P.:** SARS-CoV-2 coronavirus nucleocapsid antigen-detecting half-strip lateral flow assay toward the development of point of care tests using commercially available reagents, Anal. Chem., **92**, 11305–11309 (2020).

Please cite this article as: Çam Derin, D et al., Development of nucleic acid based lateral flow assays for SARS-CoV-2 detection, J. Biosci. Bioeng., https://doi.org/10.1016/j.jbiosc.2022.11.001